The Effect of Needle-insertion Depth on the Irrigant Flow in the Root Canal: Evaluation Using an Unsteady Computational Fluid Dynamics Model

Christos Boutsioukis, DDS, MSc,[*‡] *Theodor Lambrianidis, DDS, PhD,*[*] *Bram Verhaagen, MSc,*[§] *Michel Versluis, PhD,*[§] *Eleftherios Kastrinakis, PhD,*[†] *Paul R. Wesselink, DDS, PhD,*[‡] *and Lucas W.M. van der Sluis, DDS, PhD*[‡]

Abstract

Introduction: The aim of this study was to evaluate the effect of needle-insertion depth on the irrigant flow inside a prepared root canal during final irrigation with a syringe and two different needle types using a Computational Fluid Dynamics (CFD) model. **Methods:** A validated CFD model was used to simulate irrigant flow from either a side-vented or an open-ended flat 30-G needle positioned inside a prepared root canal (45 .06) at 1, 2, 3, 4, or 5 mm short of the working length (WL). Velocity, pressure, and shear stress in the root canal were evaluated. **Results:** The flow pattern in the apical part of the root canal was similar among different needle positions. Major differences were observed between the two needle types. The side-vented needle achieved irrigant replacement to the WL only at the 1-mm position, whereas the open-ended flat needle was able to achieve complete replacement even when positioned at 2 mm short of the WL. The maximum shear stress decreased as needles moved away from the WL. The flat needle led to higher mean pressure at the apical foramen. Both needles showed a similar gradual decrease in apical pressure as the distance from the WL increased. **Conclusions:** Needle-insertion depth was found to affect the extent of irrigant replacement, the shear stress on the canal wall, and the pressure at the apical foramen for both needle types. *(J Endod 2010;36:1664–1668)*

Key Words

Computational Fluid Dynamics, insertion depth, irrigation, needle

Irrigation of root canals with antibacterial solutions is an integral part of chemomechanical preparation, aiming at the removal of bacteria, debris, and necrotic tissue, especially from areas of the root canal that have been left unprepared by mechanical instruments (1). Irrigants are commonly delivered using a syringe and needle (2, 3), even before passive ultrasonic activation of the solution (4). The significance of the needle position in relation to the apical terminus of the preparation, also described as needle insertion depth or penetration, has been highlighted in a series of *in vitro* (5) and *ex vivo* studies (6-9). It has been hypothesized that positioning the needle close to the working length (WL) could in fact improve the debridement and irrigant replacement (6, 10). However, previous studies have mainly focused on the removal efficiency of debris and bacteria and provided little understanding of the etiology (ie, the flow pattern developed in the root canal that leads to debridement and irrigant replacement). Limited insight in the fluid dynamics of the flow inside the root canal has been presented using thermal image analysis (9) because this approach could only provide a coarse estimation of the irrigant flow.

A Computational Fluid Dynamics (CFD) model was recently introduced as a method to study root canal irrigation (11). This model was subsequently validated by comparison with experimental high-speed imaging data (12) and used to evaluate the effect of needle tip design on the flow (13). In these previous studies, needles were positioned at 3 mm short of the WL. A similar approach has also been reported (14, 15), but the effect of needle insertion depth on the irrigant flow has not been studied in detail. The aim of this study was to evaluate the effect of needle insertion depth on the irrigant flow inside a prepared root canal during final irrigation with a syringe and two different needle types using the validated CFD model.

Materials and Methods

The root canal and apical anatomy were simulated similarly to a previous study (11), assuming a length of 19 mm, an apical diameter of 0.45 mm (ISO size 45), and 6% taper. The apical foramen was simulated as a rigid and impermeable wall, corresponding to a closed system.

Two different needle types, a side-vented and an open-ended flat needle, were modeled using commercially available 30-G needles as references, similar to a previous study (13). The external and internal diameter and the length of the needles were stan-

From the *Department of Endodontology, Dental School and [†]Chemical Engineering Department, School of Engineering, Aristotle University of Thessaloniki, Thessaloniki, Greece; [‡]Department of Cariology Endodontology Pedodontology, Academic Centre for Dentistry Amsterdam (ACTA), Amsterdam, The Netherlands; and [§]Physics of Fluids Group, Faculty of Science and Technology, and Research Institute for Biomedical Technology and Technical Medicine MIRA, University of Twente, Enschede, The Netherlands.

Supported in part by a Scholarship for Excellent PhD Students from the Research Committee of Aristotle University of Thessaloniki, Greece (CB), and through Project 07498 of the Dutch Technology Foundation STW (BV).

Address requests for reprints to Mr Christos Boutsioukis, 29, Kimis Str, 551 33 Thessaloniki, Greece. E-mail address: chb@dent.auth.gr.

0099-2399/$0 - see front matter

doi:10.1016/j.joen.2010.06.023

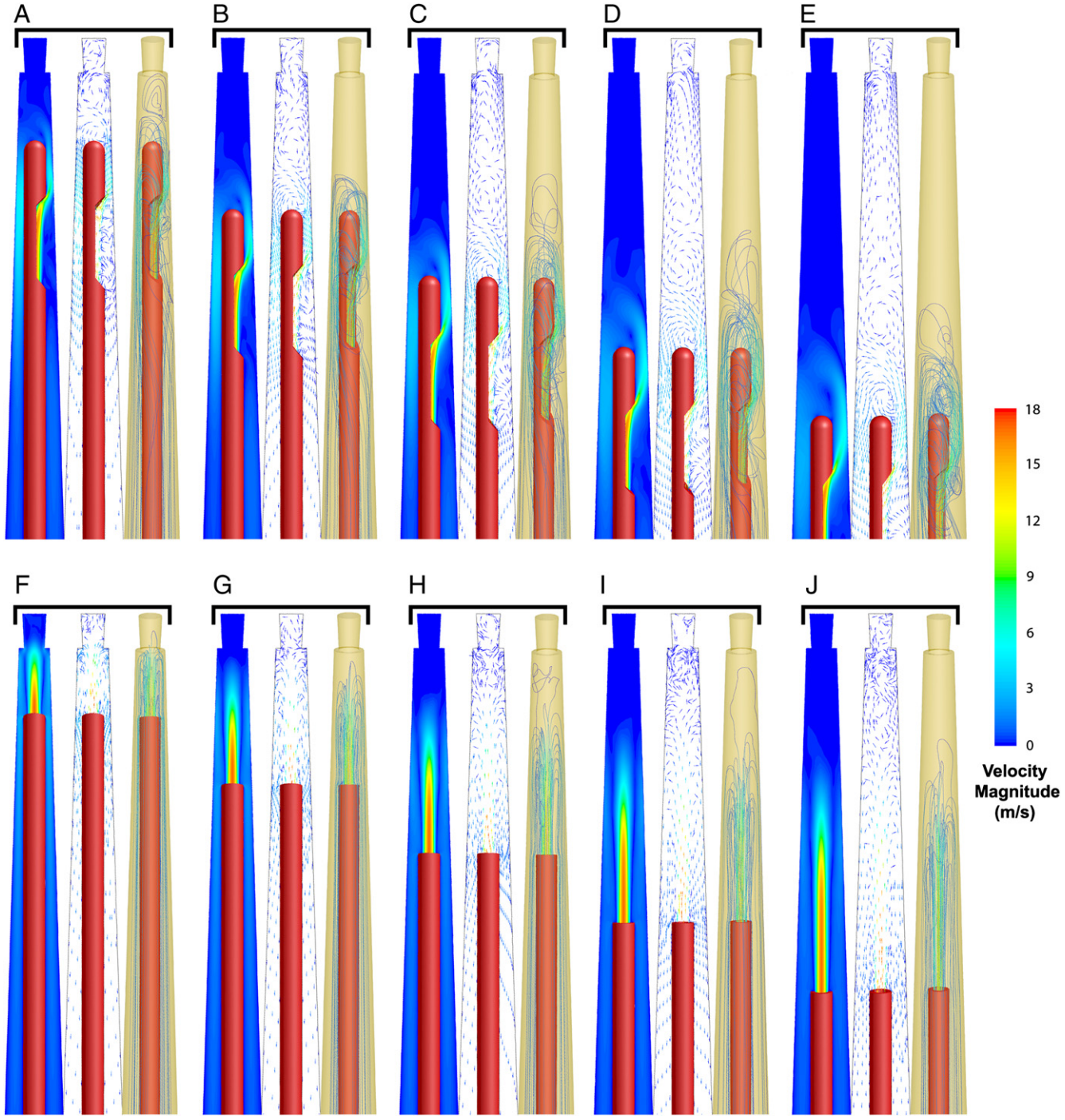

Figure 1. Triads of time-averaged contours of velocity magnitude (*left*) and vectors (*middle*) along the *z-y* plane in the apical part of the root canal and streamlines indicating the route of mass-less particles released downstream from the needle inlet and colored according to the time-averaged velocity magnitude (*right*) for the (*A-E*) side-vented and (*F-J*) flat needle positioned at 1 to 5 mm short of the WL, respectively. Particle trajectories provide visualization of the fresh irrigant main flow in three dimensions. (*A-E*) A series of counter-rotating vortices (flow structures where the fluid is rotating) apically to the side-vented needle was identified regardless of needle position. The size and position of the vortices varied, and the number or vortices increased as the needle was positioned further away from the WL. (*F-J*) A high-velocity jet of irrigant along the longitudinal axis of the root canal (*z*-axis) was identified apically to the flat needle, which extended even further than the apical constriction in the 1-mm case. The jet appeared to break up gradually because of the recirculating flow and damping by the irrigant already present in the canal. Jets extended longer away from the tip of the needle as the needle moved further away from the WL. Needles are colored in red. (This figure is available in color online at www.aae.org/joe/.)

dardized (D_{ext} = 320 μm, D_{int} = 196 μm, and l = 31 mm, respectively). The needles were fixed and centered within the canal. Five different depths were simulated for each needle type, namely 1, 2, 3, 4, and 5 mm short of the WL.

The preprocessor software Gambit 2.4 (Fluent Inc, Lebanon, NH) was used to build the three-dimensional geometry and the mesh. A hexahedral mesh was constructed and refined near the walls and in the areas in which high gradients of velocity were anticipated, such as

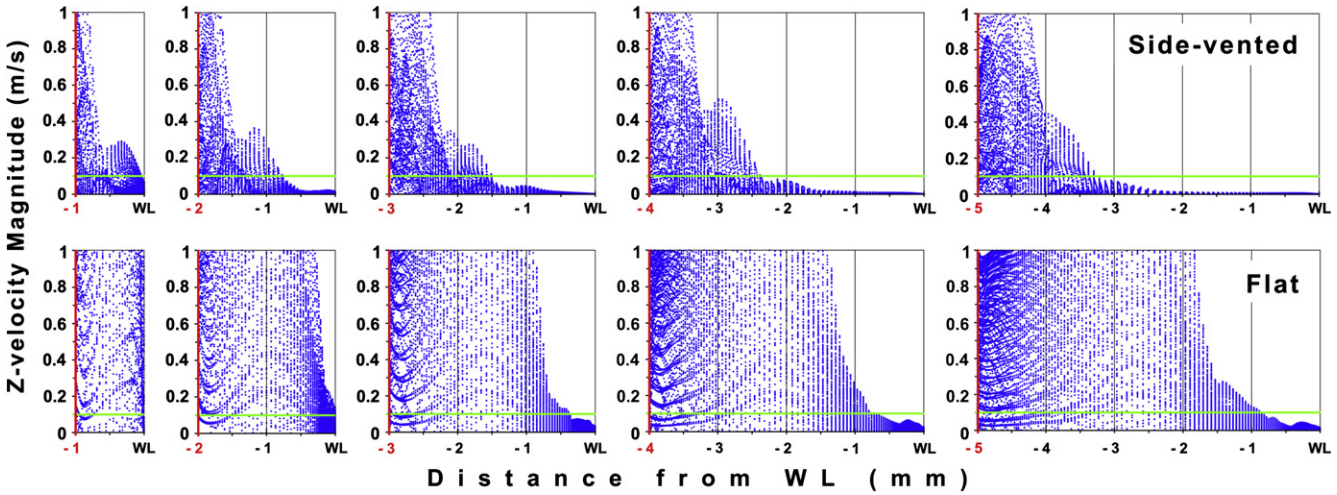

Figure 2. The distribution of the axial z-component of time-averaged irrigant velocity in the apical part of the canal as a function of distance from the WL for the (*top*) side-vented and the (*bottom*) flat needle. The position of the needle is depicted by the vertical red line. The scale of the vertical axis has been adjusted to 0 to 1 m/s to highlight differences in the area apically to the needle tips. Velocities higher than 0.1 m/s (horizontal green line) were considered clinically significant for adequate irrigant replacement. Irrigant flow coronally to the outlet showed complete replacement in these parts of the canal irrespective of the needle type or depth. (This figure is available in color online at www.aae.org/joe/.)

near the needle outlet. A grid-independency check was performed to ensure the reasonable use of computational resources. The final meshes consisted of 496,000 to 708,000 cells depending on the needle type and position (mean cell volume, $2.4\text{-}3.4 \cdot 10^{-5}$ mm^3).

No-slip boundary conditions were imposed on the walls of the root canal and of the needles under the hypothesis of rigid, smooth, and impermeable walls. The fluid flowed into the simulated domain through the needle inlet and out of the domain through the root canal orifice where atmospheric pressure was imposed. The canal and needle were assumed to be completely filled with irrigant. A flat velocity profile with a constant axial velocity of 8.6 m/s was imposed at the inlet, which is consistent with a clinically realistic irrigant flow rate of 0.26 mL/s through a 30-G needle (16). The irrigant, sodium hypochlorite 1% aqueous solution, was modeled as an incompressible, Newtonian fluid with density $\rho = 1.04$ g/cm^3 and viscosity $\mu = 0.99 \cdot 10^{-3}$ Pa·s (17). Gravity was included in the flow field in the direction of the negative z axis.

The commercial CFD code FLUENT 6.3 (Fluent Inc) was used to set up and solve the problem. Detailed settings of the solver can be found in a previous study that assessed the validity of the model used (12). An unsteady isothermal flow was assumed. No turbulence model was used because the flow under these conditions was expected to be laminar (11, 12). A time step of 10^{-6} was used throughout the calculations, which were carried out for a real flow time of 50 milliseconds for each case. Computations were performed in a computer cluster (45 dual-core AMD Opteron 270 processors [Advanced Micro Devices, Sunnyvale, CA]) running 64-bit SUSE Linux 10.1 (kernel version 2.6.16). The flow fields computed were compared in terms of flow pattern, velocity magnitude, shear stress, and apical pressure.

Results

An unsteady flow (nonstationary) was identified in all cases, regardless of needle type or insertion depth. The time-averaged flow pattern in the apical part of the canal presented slight differences among the various needle positions for both needle types. However, major differences were observed between the two needle types (Fig. 1).

Analysis of the axial z-component of irrigant velocity in the apical part of the root canal as a function of distance from the WL provided a detailed overview of irrigant replacement (Fig. 2), which was considered clinically significant for velocities higher than 0.1 m/s (13). The side-vented needle appeared to achieve adequate irrigant replacement within 1 to 1.5 mm apically to its tip regardless of position. Only the 1-mm position presented adequate replacement to the WL. The flat needle led to a more extensive irrigant exchange apically to its tip, which reached the WL in 1- and 2-mm positions.

The shear stress pattern on the canal wall was similar among the different positions of the same needle (Fig. 3.1). The maximum shear stress decreased as needles moved away from the WL, but the area affected by high shear stress became larger. This area always surrounded the tip of the side-vented needle with maximum shear stress concentrated on the wall facing the needle outlet. For the open-ended flat needle, high shear stress was identified apically to its tip.

Pressure developed at the apical foramen differed among the various positions and needle types (Fig. 3.2). The flat needle led to higher mean pressure at the apical foramen than the side-vented needle at the same depth.

Discussion

In a previous study evaluating the effect of needle type on irrigant flow, two main groups of needles were identified, namely, the closed-ended and the open-ended groups (13). In the present study, one needle type from each one of the two groups was selected to evaluate the effect of needle depth on the two different flow patterns and also to allow comparison with previous studies. For both needles tested in this study, the depth of placement appeared to have a limited influence on the general characteristics of the flow pattern developed.

A change in the needle-insertion depth resulted in a change in both the distance between the needle tip and the WL and in the proximity of the needle tip to the lateral canal wall. The present study design did not allow the evaluation of each one of these changes separately and the results reported could be attributed to both changes. However, these two factors usually cannot be isolated during clinical practice. Thus, the current study design aimed to evaluate clinically realistic options

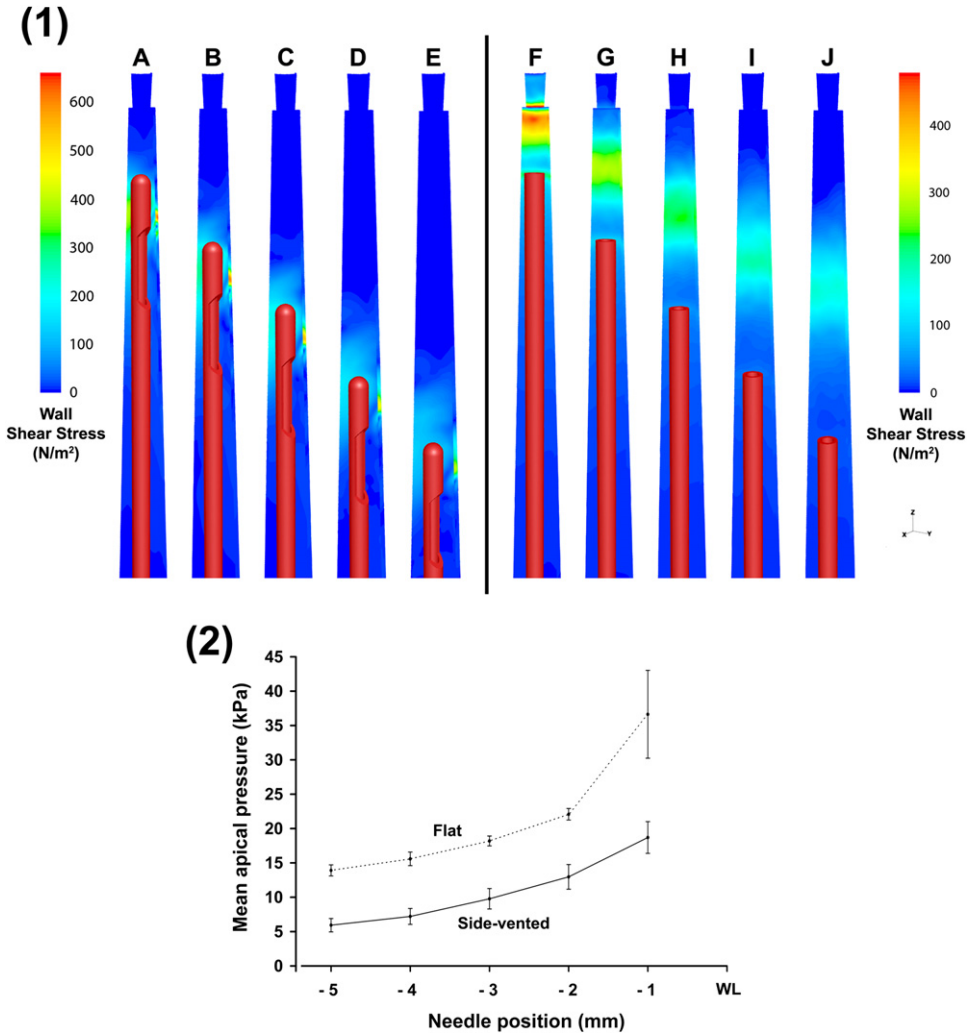

Figure 3. (*1*) The time-averaged distribution of shear stress on the root canal wall for the (*A-E*) side-vented and (*F-J*) flat needle positioned at 1 to 5 mm short of the WL, respectively. Only half of the root canal wall is presented to allow simultaneous evaluation of the needle position. A maximum shear stress of 660 N/m^2 for the side-vented needle and 480 N/m^2 for the flat needle was noticed at the 1-mm cases. Needles are colored in red. (*2*) Time-averaged irrigant pressure at the apical foramen developed by the side-vented and the flat needle as a function of needle position (distance from the WL). Data shown as mean ± standard deviation. Both needles showed a similar gradual decrease in apical pressure as the distance from the WL increased, except from the decrease between 1- and 2-mm positions for the flat needle in which a sharp decrease of 14.6 kPa (40% of the mean apical pressure) was noted. The pressure developed by the side-vented needle when positioned at 1 mm was comparable to the pressure developed by the flat needle positioned at 3 mm. (This figure is available in color online at www.aae.org/joe/.)

regarding the positioning of the needle. The effect of the space available between the needle and the lateral canal wall will be evaluated in a separate study using a different design.

In the present study, a closed system was modeled according to a previously published definition (18), which more closely resembles the situation *in vivo*. It has been reported that in such a system there is a possibility of air bubble entrapment in the apical part of the root canal during irrigation (18), which could impede irrigant penetration and replacement and root canal debridement (18). However, in that study, an irrigant flow rate of 0.083 mL/s was used, which is low compared with previous reports (8, 16). The importance of the flow rate for the irrigant flow in the root canal has been shown previously (11). In the present study, a flow rate of 0.26 mL/s was used for all cases in accordance to a previous *ex vivo* study (16). This flow rate can be reached by using a 5-mL syringe instead of a 10-mL syringe. In a pilot CFD study, it was concluded that the irrigant flow rate also affects the entrapment and the size of an air bubble in the apical part of the root canal. The extent of air bubble entrapment was very limited when a flow rate of 0.26 mL/s was used (data not shown). Therefore, the effect of bubble entrapment was neglected in the simulations reported in the present study, and the root canal was assumed to be completely filled with the irrigant in all cases.

The relevance of the *z*-velocity magnitude; the shear stress; and the apical pressure to irrigant replacement, mechanical debridement, and irrigant extrusion has been analyzed previously (13). The general trend that needle placement closer to the WL resulted in more efficient irrigant replacement, as identified in the present study, is consistent with the results of previous studies (5, 8, 9). More effective *ex vivo* removal of bioluminescent bacteria from root canals has been reported when a side-vented needle was placed at 1 mm short of the WL rather than at 5 mm (8). That study mainly assessed the ability to exchange the irrigant in the root canal rather than the ability to detach microbes from the canal wall because the bioluminescent bacteria were in suspension. However, the difference was statistically significant only when 6 mL of

irrigant was delivered, not with 3 mL. It is unlikely that the removal of bacteria was similar for 1- and 5-mm positions regardless of the volume of irrigant delivered. In the vertical vortex structure developed apically to the side-vented needle, some degree of irrigant exchange is expected, but velocities drop significantly from vortex to vortex toward the apex (19). Because the needle is positioned further away from WL, the increased number of vortices causes a delay in the irrigant replacement. A higher volume of irrigant, which has been shown to affect the irrigation efficiency (20), can be translated to an increased duration of irrigation when the flow rate is constant according to the definition of flow rate (Q): $Q = \frac{\Delta V}{\Delta t}$, where ΔV is the volume of fluid crossing the control surface (in this case delivered through the needle) during the specified time period (Δt) (21). An increased duration of irrigation is expected to improve irrigant exchange in all cases, regardless of needle position, magnifying any existing difference. It is possible that limited resolution of the acquired images (8) caused a lack of significant difference in the 3-mL group. Results from the 6-mL group are in agreement to the findings of the present study although root canal geometry, needle size, and flow rate were slightly different.

In another study using thermal image analysis (9), it was shown that the flow apically to a beveled needle reached the apex when the needle was placed at 3 mm short of the WL but not when it was placed at 6 mm. It has been reported that the flat and beveled needle produce similar flow patterns in root canals (13); therefore, these results are comparable to the results of the present study using the flat needle. Minor differences in the taper and needle size or the limited resolution achieved by the infrared camera may account for a 0.3-mm difference in the extent of apical irrigant replacement at the 3-mm position between the two studies.

According to the results of the present study, positioning of the needle closer to the WL improved the irrigant replacement in the apical part of the root canal (indicated by a high axial z-component of velocity) but also led to increased mean pressure at the apical foramen, indicating an increased risk of irrigant extrusion toward the periapical tissue. The requirements of adequate irrigant replacement and reduced apical pressure appeared to contradict each other. From a clinical point of view, the prevention of extrusion should precede the requirement for adequate irrigant replacement and wall shear stress. However, because there is no definite evidence on the minimum irrigant pressure that leads to extrusion, the risk of extrusion can only be estimated by comparison between different needle positions.

Irrigant replacement reached the WL only when the side-vented needle was placed at 1 mm; therefore, it seems reasonable to suggest that this needle should be positioned within 1 mm from the WL if possible. Additional safety against irrigant extrusion in case of binding in the root canal is provided by the blind end of the side-vented needle. On the other hand, the flat needle and probably also similar types like the notched or the beveled needle (13) should not be placed at 1 mm because of the high apical pressure developed. This pressure is likely to be even higher when the root canal is smaller and no safety feature like a blind-end needle is available to prevent forceful extrusion in case of binding. The further the needle is positioned away from the WL, the less apical pressure is developed, but then the irrigant exchange is also less efficient and wall shear stress is lower. A reasonable compromise would be the 2- or 3-mm position, which still ensures adequate irrigant exchange. The optimal needle depth may be also influenced by canal size and taper and the presence of a curvature. The importance of these additional factors should be assessed in future studies.

In conclusion, needle-insertion depth was found to affect the extent of irrigant replacement, the shear stress on the canal wall, and the pressure at the apical foramen.

Acknowledgments

The authors are grateful to B. Benschop for technical assistance.

References

1. Gulabivala K, Patel B, Evans G, et al. Effects of mechanical and chemical procedures on root canal surfaces. Endod Top 2005;10:103–22.
2. Ingle JI, Himel VT, Hawrish CE, et al. Endodontic cavity preparation. In: Ingle JI, Bakland LK, eds. Endodontics. 5th ed. Ontario, Canada: BC Decker; 2002:502.
3. Peters OA. Current challenges and concepts in the preparation of root canal systems: a review. J Endod 2004;30:559–67.
4. van der Sluis LWM, Gambarini G, Wu MK, et al. The influence of volume, type of irrigant and flushing method on removing artificially placed dentine debris from the apical root canal during passive ultrasonic irrigation. Int Endod J 2006;39:472–6.
5. Chow TW. Mechanical effectiveness of root canal irrigation. J Endod 1983;9:475–9.
6. Abou-Rass M, Piccinino MV. The effectiveness of four clinical irrigation methods on the removal of root canal debris. Oral Surg Oral Med Oral Pathol 1982;54:323–8.
7. Albrecht LJ, Baumgartner JC, Marshall JG. Evaluation of apical debris removal using various sizes and tapers of ProFile GT files. J Endod 2004;30:425–8.
8. Sedgley CM, Nagel AC, Hall D, et al. Influence of irrigant needle depth in removing bacteria inoculated into instrumented root canals using real-time imaging in vitro. Int Endod J 2005;38:97–104.
9. Hsieh YD, Gau CH, Kung Wu SF, et al. Dynamic recording of irrigating fluid distribution in root canals using thermal image analysis. Int Endod J 2007;40:11–7.
10. Zehnder M. Root canal irrigants. J Endod 2006;32:389–98.
11. Boutsioukis C, Lambrianidis T, Kastrinakis E. Irrigant flow within a prepared root canal using different flow rates: a computational fluid dynamics study. Int Endod J 2009;42:144–55.
12. Boutsioukis C, Verhaagen B, Versluis M, et al. Irrigant flow in the root canal: experimental validation of an unsteady computational fluid dynamics model using high-speed imaging. Int Endod J 2010;43:393–403.
13. Boutsioukis C, Verhaagen B, Versluis M, et al. Evaluation of irrigant flow in the root canal using different needle types by an unsteady computational fluid dynamics model. J Endod 2010;36:875–9.
14. Gao Y, Haapasalo M, Shen Y, et al. Development and validation of a three-dimensional computational fluid dynamics model of root canal irrigation. J Endod 2009;35:1282–7.
15. Shen Y, Gao Y, Qian W, et al. Three-dimensional numeric simulation of root canal irrigant flow with different irrigation needles. J Endod 2010;36:884–9.
16. Boutsioukis C, Lambrianidis T, Kastrinakis E, et al. Measurement of pressure and flow rates during irrigation of a root canal ex vivo with three endodontic needles. Int Endod J 2007;40:504–13.
17. Guerisoli DMZ, Silva RS, Pecora JD. Evaluation of some physico-chemical properties of different concentrations of sodium hypochlorite solutions. Braz Endod J 1998;3:21–3.
18. Tay FR, Gu LS, Schoeffel GJ, et al. Effect of vapor lock on root canal debridement by using a side-vented needle for positive-pressure irrigant delivery. J Endod 2010;36:745–50.
19. Shankar PN, Deshpande MD. Fluid mechanics in the driven cavity. Annu Rev Fluid Mech 2000;32:93–136.
20. Sedgley C, Applegate B, Nagel A, et al. Real-time imaging and quantification of bioluminescent bacteria in root canals in vitro. J Endod 2004;30:893–8.
21. Hughes WF, Brighton JA. Fluid Dynamics. 3rd ed. New York: McGraw-Hill; 1999:2–6, 34–61, 118–23, 245–6.